Physics Letters B 701 (2011) 180–185

Contents lists available at ScienceDirect

Physics Letters B

www.elsevier.com/locate/physletb

Observation of parametric X-rays produced by 400 GeV/c protons in bent crystals

W. Scandale [a,b], G. Arduini [a], R. Assmann [a], F. Cerutti [a], S. Gilardoni [a], J. Christiansen [a], E. Laface [a], R. Losito [a], A. Masi [a], E. Metral [a], D. Mirarchi [a], S. Montesano [a], V. Previtali [a], S. Redaelli [a], G. Valentino [a], P. Schoofs [a], G. Smirnov [a], L. Tlustos [a], E. Bagli [c], S. Baricordi [c], P. Dalpiaz [c], V. Guidi [c], A. Mazzolari [c], D. Vincenzi [c], B. Buonomo [d], S. Dabagov [d], F. Murtas [d], A. Carnera [e], G. Della Mea [e], D. De Salvador [e], A. Lombardi [e], O. Lytovchenko [e], M. Tonezzer [e], G. Cavoto [f], L. Ludovici [f], R. Santacesaria [f], P. Valente [f], F. Galluccio [g], A.G. Afonin [h], M.K. Bulgakov [h], Yu.A. Chesnokov [h], V.A. Maisheev [h], I.A. Yazynin [h], A.D. Kovalenko [i], A.M. Taratin [i,*], Yu.A. Gavrikov [j], Yu.M. Ivanov [j], L.P. Lapina [j], V.V. Skorobogatov [j], W. Ferguson [k], J. Fulcher [k], G. Hall [k], M. Pesaresi [k], M. Raymond [k], A. Rose [k], M. Ryan [k], O. Zorba [k], G. Robert-Demolaize [l], T. Markiewicz [m], M. Oriunno [m], U. Wienands [m], Yu.V. Efremov [n], S.R. Uglov [o], A.S. Gogolev [o]

[a] CERN, European Organization for Nuclear Research, CH-1211 Geneva 23, Switzerland
[b] Laboratoire de l'Accelerateur Lineaire (LAL), Université Paris Sud Orsay, Orsay, France
[c] INFN Sezione di Ferrara, Dipartimento di Fisica, Università di Ferrara, Ferrara, Italy
[d] INFN LNF, Via E. Fermi, 40 00044 Frascati (Roma), Italy
[e] INFN Laboratori Nazionali di Legnaro, Viale Università 2, 35020 Legnaro (PD), Italy
[f] INFN Sezione di Roma, Piazzale Aldo Moro 2, 00185 Rome, Italy
[g] INFN Sezione di Napoli, Italy
[h] Institute of High Energy Physics, RU-142284 Protvino, Moscow Region, Russia
[i] Joint Institute for Nuclear Research, Joliot-Curie 6, 141980 Dubna, Moscow Region, Russia
[j] Petersburg Nuclear Physics Institute, 188300 Gatchina, Leningrad Region, Russia
[k] Imperial College, London, United Kingdom
[l] Brookhaven National Laboratories, P.O. Box 5000 Upton, NY 11973-5000, USA
[m] SLAC National Accelerator Laboratory, 2575 Sand Hill Road, Menlo Park, CA 94025, USA
[n] Institute in Physical and Technical Problems, 141980 Dubna, Moscow Region, Russia
[o] Institute of Physics and Technology at TPU, 634050 Tomsk, Russia

ARTICLE INFO

Article history:
Received 15 March 2011
Received in revised form 22 April 2011
Accepted 2 May 2011
Available online 30 May 2011
Editor: W.-D. Schlatter

Keywords:
Crystal
Proton
Parametric X-ray radiation

ABSTRACT

Spectral maxima of parametric X-ray radiation (PXR) produced by 400 GeV/c protons in bent silicon crystals aligned with the beam have been observed in an experiment at the H8 external beam of the CERN SPS. The total yield of PXR photons was about 10^{-6} per proton. Agreement between calculations and the experimental data shows that the PXR kinematic theory is valid for bent crystals with sufficiently small curvature as used in the experiment. The intensity of PXR emitted from halo protons in a bent crystal used as a primary collimator in a circular accelerator may be considered as a possible tool to control its crystal structure, which is slowly damaged because of irradiation. The intensity distribution of PXR peaks depends on the crystal thickness intersected by the beam, which changes for different orientations of a crystal collimator. This dependence may be used to control crystal collimator alignment by analyzing PXR spectra produced by halo protons.

1. Introduction

Parametric X-ray radiation (PXR) is emitted by a fast charged particle in a crystal due to diffraction of its virtual-photon field on crystallographic planes. PXR has been theoretically predicted [1–3] and then observed and studied using electron beams of different energies [4,5]. The first experiment with the aim of PXR observation from heavy charged particles was carried out on the 70 GeV proton beam at IHEP [6]. Recently, PXR has been successfully observed from 5 GeV protons and 2.2 GeV/u carbon nuclei in a silicon crystal on the external beams of the Nuclotron at LHE JINR [7,8].

* Corresponding author.
E-mail address: alexander.taratin@cern.ch (A.M. Taratin).

0370-2693/$ – see front matter
doi:10.1016/j.physletb.2011.05.060

The characteristics of PXR are determined by the particle velocity v and they are independent of the charge sign and mass of the particle. The energy of PXR photons generated by a particle in a crystal at the angle θ relative to its velocity is determined as [1]

$$E_n = n\hbar c \frac{\vec{g}\cdot\vec{\beta}}{1-\sqrt{\varepsilon_o}\beta\cos\theta},$$

where n is the diffraction order, $\vec{g}$ is the reciprocal lattice vector, $\beta = v/c$ and ε_o is the constant part of the medium permittivity ($\varepsilon_o \approx 1$ for X-rays). The experimental test of this formula was performed in [9]. The PXR photon energies generated on the fixed crystal planes may be calculated using the following detailed expression of the formula

$$E_n = n\hbar\omega_1 = n\frac{2\pi\hbar c}{d}\frac{\beta\sin\theta_B}{1-\sqrt{\varepsilon_o}\beta\cos\theta_D\cos\theta_y}, \quad (1)$$

where d is the interplanar distance, θ_B is the orientation angle of the crystal planes with respect to the particle momentum, θ_D and θ_y are the radiation detection angles in the diffraction plane formed by $\vec{g}$ and $\vec{\beta}$ and in the normal plane, respectively. The direction of the PXR maximum is determined by the angle $\theta_D = 2\theta_B$ and $\theta_y(\omega) = \sqrt{\gamma^{-2} + (\omega_p/\omega)^2}$, where γ is the relativistic Lorentz factor of the particles and $\hbar\omega_p = 31$ eV is the plasmon energy in silicon.

The PXR generated by channeled particles in bent crystals has been considered in [10] where the possibility of the PXR focusing was discussed. The application of PXR for online diagnostics of the beam and the bent crystal state was proposed in [11]. Recently [12], it was suggested to use PXR to control the state of the crystal deflector during its use for beam extraction and collimation in high energy accelerators, which is slowly changed because of defects produced by irradiation. Studies using a bent crystal as a primary collimator for the Large Hadron Collider (LHC) are under way now at the CERN Super Proton Synchrotron (SPS) [13]. The control of the structure state of a primary crystal collimator is important because of its high irradiation by a growing collider halo.

In this Letter the results of PXR observation from 400 GeV/c protons in bent silicon crystals in the collimation geometry at the H8 external beam of the CERN SPS are presented.

2. The experimental layout

Fig. 1 shows the experimental layout in the horizontal plane. The figure parts (a) and (b) are for the experiments with quasi-mosaic (QM) and strip (ST) crystals, respectively, produced according to the methods described in [14–16]. The beam entered the crystal in the collimation geometry such that it is parallel to the deflecting planes, which are the (111) and (110) crystallographic planes for the QM and ST crystals, respectively. A high precision goniometer was used to orient the crystal planes with respect to the beam axis with an accuracy of 2 μrad. The accuracy of the preliminary crystal alignment using a laser beam was about 0.1 mrad. Five pairs of microstrip silicon detectors S_1–S_5, two upstream and three downstream of the crystal, were used to measure incoming and outgoing angles of particles with an angular resolution in each arm of about 3 μrad. The divergence of the incident beam measured with the detector telescope was characterized by the RMS deviations $\sigma_x = 10.7$ μrad and $\sigma_y = 7.6$ μrad [17]. The scintillation detector S_c downstream of the silicon telescopes was used as a trigger. It registered the number of protons in the beam N_o with an accuracy of about 10%. The average cycle time of the SPS during the measurements was about 45 s with the pulse duration 10–11 s and the average number of particles per spill about $(1.3 \pm 0.1) \times 10^6$.

PXR generated due to diffraction of virtual photons of proton field on the (110) and (100) crystallographic planes ("radiating planes") in the case of (a) and (b) shown in Fig. 1, respectively, was registered by the X-ray detector D. The inclination angles of these radiating planes relative to the deflecting ones and hence with the beam were $\theta_B = 35.26°$ (a) and 45° (b). The X-ray detector was placed close to the PXR maximum direction, $\theta_D = 2\theta_B$, the detection angles θ_D were 70.25° and 90° in the cases (a) and (b), respectively. So, the real detector position in the case (a) was shifted a little from the Bragg angle $\theta_D = 70.52°$.

The semiconductor silicon detector D used for detection of PXR photons is 380 μm thick with a sensitive surface area of about 13 mm^2 and with a 25 μm beryllium window. The distance between the crystal and detector was changed in the range $S_d = (95–127)$ mm. The detector D was placed in a cavity inside a lead brick to reduce the radiation background. The crystal was seen by the detector through a collimating window of 5 mm diameter and 50 mm length. The semiconductor detector was calibrated by using the lines of characteristic radiation excited in a copper target by the proton beam (see [7]). The energy resolution of the detector for the 8.046 keV K_α line was equal to about 250 eV. The detector efficiency is close to 100% for photons with energies 4–8 keV and it reduces with further increase of photon energy. The efficiency estimated using the photoabsorption cross-section in silicon was used to compare the experimental results with the PXR theory.

3. PXR generated in QM crystal deflector

The QM crystal $40 \times 30 \times 2$ mm^3 (Height × Width × Thickness) used for the PXR measurements in the case (a) was mechanically bent along its height and placed with its thickness parallel to the beam. The QM curvature produced along the thickness and hence along the (111) planes with bend radius $R = 17.4$ m was used for beam deflection in the horizontal plane. The crystal position in the beam can be determined from Fig. 2a where the beam intensity behind the crystal is shown as a function of the incident horizontal coordinate X and the proton deflection angle. The crystal has also an anticlastic curvature along its width, which changes the orientation of the (111) planes with X. Therefore, the edge of the crystal deflected protons due to channeling and deeper crystal layers deflected them in the opposite direction due to volume reflection. Fig. 2b shows the incident beam distribution in the horizontal coordinate X where the crystal edge is shown by the dashed line. The PXR detector is on the left of the crystal at a distance $S = 117$ mm as shown in Fig. 1.

The energies of PXR photons of different diffraction order n in case (a) calculated according to (1) are equal to $E_n = n \times E_1$ with $E_1 = 5.59$ keV. Fig. 3a shows the radiation spectrum measured by the detector. Three peaks are seen above the background, which was fitted by a fourth order polynomial function shown by the blue curve. Fig. 3b shows the spectrum after background subtraction. The PXR peaks were fitted by Gaussians. The fit parameters, which determine the peak center M, are presented in Table 1. The peak positions are in excellent agreement with the PXR energies E_n determined by (1). The number of photons $N_{\gamma n}$ registered in the peaks are given in Table 1. The total number of protons in the beam N_o and the beam fraction which passed through the crystal during the PXR measurements, $F_{cr} = 0.77 \pm 0.02$ obtained from Fig. 2, allowed to determine the PXR yields per proton I_γ. The PXR yields and their ratio $I_{\gamma 1}/I_{\gamma n}$ are also presented in Table 1. The errors of I_γ values are mainly caused by the errors of N_γ and by the error of N_o, which was estimated to be about 10% as it was mentioned above. The total registered yield of PXR is larger than 10^{-6} photon/p. More than half of the detected photons are the

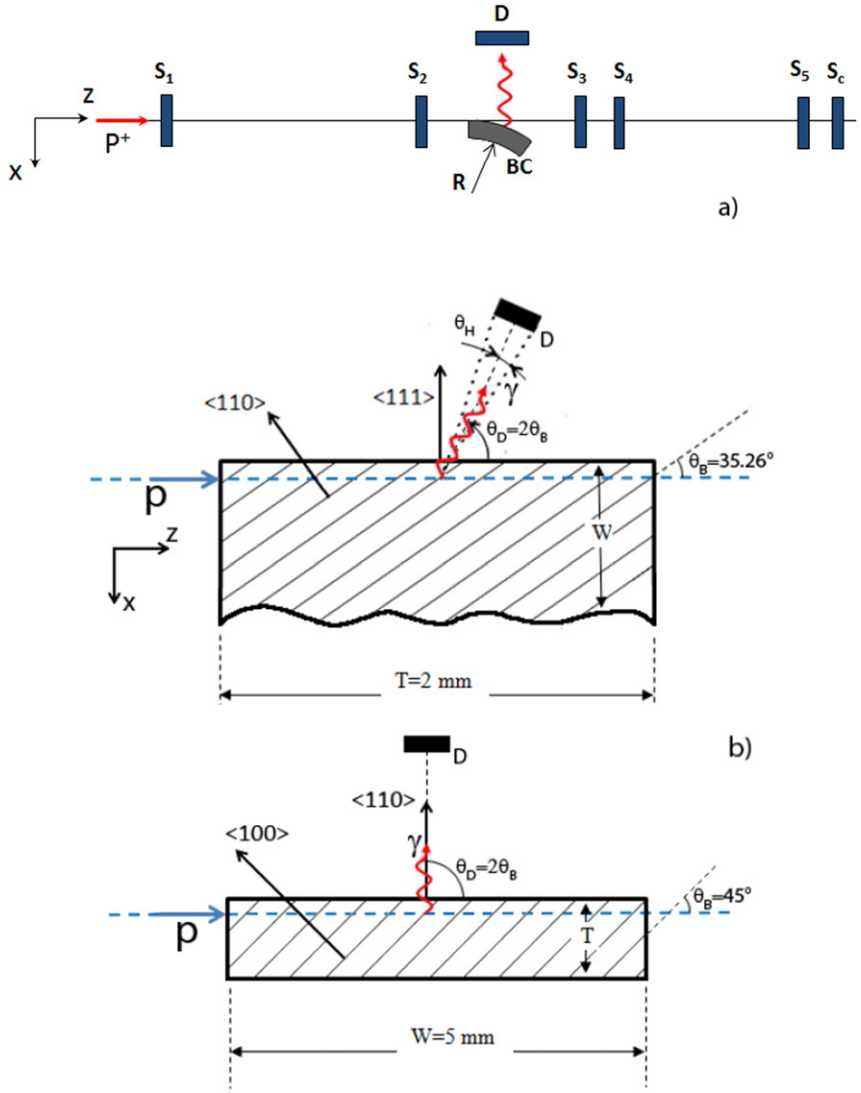

Fig. 1. (Color online.) A schematic view from below of the layout of the experiment for the observation of parametric radiation produced by protons in bent silicon crystals BC in the horizontal plane. S_1–S_5 are the silicon microstrip detectors, S_c is the scintillation trigger. The experiment details: (a) for quasi-mosaic crystal, (b) for strip crystal. The beam enters the crystal parallel to the (111) and (110) deflecting planes for (a) and (b) cases, respectively. The crystal bend is small and is not shown. PXR photons are produced due to diffraction of virtual photons of the proton field on the (110) and (100) planes for (a) and (b) cases, respectively. Photon angles θ_H are measured from the direction θ_D of the PXR maximum.

Table 1
PXR characteristics for QM crystal.

Reflex	M (keV)	N_γ	I_γ (10^{-7})	$I_{\gamma 1}/I_{\gamma n}$	Theory I_γ (10^{-7})	Theory $I_{\gamma 1}/I_{\gamma n}$
1	5.58 ± 0.01	420 ± 20	6.9 ± 0.8	1	4.35	1
2	11.18 ± 0.01	230 ± 16	3.8 ± 0.4	1.8 ± 0.3	3.33	1.3
3	16.70 ± 0.06	47 ± 8	0.77 ± 0.12	9 ± 2	0.69	6.3

first diffraction order ones because the detector is sufficiently close and soft photon absorption in the air is small.

4. PXR generated in ST crystal deflector

The strip crystal $70 \times 5 \times 2$ mm^3 (Height × Width × Thickness) with its largest faces parallel to the (110) planes was used for the PXR measurements in the case (b) and was mechanically bent along its height. The anticlastic bending produced along the crystal width, which had $R = 33.3$ m, was used for beam deflection in the horizontal plane (see the crystal figure in Fig. 2b in [18]). The bend radii for the crystals used in our experiment are much larger than the critical value R_c for particle channeling ($R_c = 68$ cm for the (110) silicon planes). Fig. 4 shows similar data to Fig. 2, giving information about the position of the strip crystal in the beam. The crystal was in an amorphous orientation and deflected protons only due to multiple Coulomb scattering. The left and right crystal edges are shown by dashed lines. The beam fraction which passed through the crystal is about $F_{cr} = 0.62 \pm 0.02$. The PXR detector is on the left of the crystal at the distance $S = 127$ mm.

The energies of PXR photons in case (b) calculated according to (1) are equal to $E_n = n \times E_1$ with $E_1 = 6.46$ keV. Fig. 5(top) shows the spectrum observed in this case after background subtraction. Only two peaks are visible here. They were also fitted by

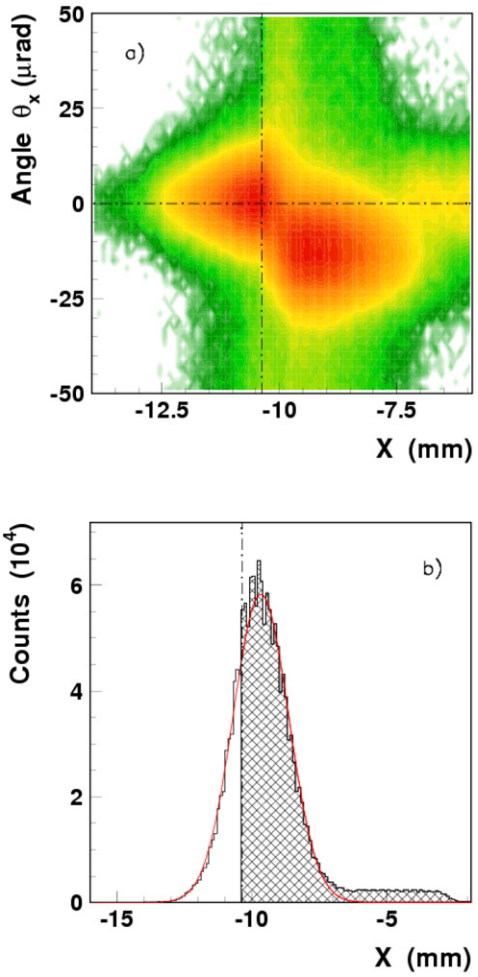

Fig. 2. (Color online.) (a) Intensity of the beam crossing the QM crystal location as a function of the incident horizontal coordinate X and the deflection angle of the protons. The fraction of the beam on the left of the dashed line missed the crystal. The edge of the crystal deflected the protons due to channeling, and deeper crystal layers on the right deflected them in the opposite direction due to volume reflection. (b) The incident beam distribution in the horizontal coordinate X. The crystal edge is shown by the dashed line. The hatched area shows the fraction of the beam intersected by the crystal. The PXR detector is on the left of the crystal.

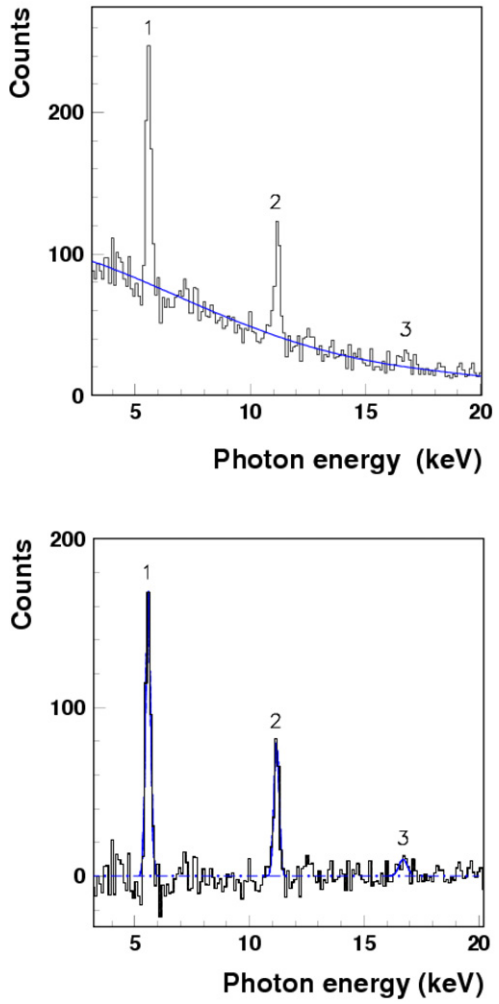

Fig. 3. (Color online.) (a) X-ray spectrum recorded by the semiconductor detector during the irradiation of the QM crystal by the proton beam. The blue line shows the fit of the background with a fourth order polynomial function. (b) PXR spectrum after background subtraction. Blue lines show Gaussian fits to the PXR peaks. Numbers in the plots correspond to the diffraction order for the peaks.

Gaussians and Table 2 presents the measured PXR parameters. The peak positions are in good agreement with the PXR energies E_n calculated according to (1). The PXR yield is more than two times smaller than for the QM crystal because the (100) planes have a lower atomic density and hence a lower density of electrons which scatter the virtual photons of the proton field.

The measurements were also performed for another thinner strip crystal (0.4 mm thick) in the channeling condition. Fig. 5(bottom) shows the recorded spectrum after background subtraction. The second peak becomes less visible compared to the results shown in Fig. 5(top) for the thicker crystal. This is readily understandable because the attenuation length for photons with energy E_2 in silicon is about 270 μm, which is already comparable with the crystal thickness. The measured parameters of PXR are presented in Table 3. The PXR intensity was not estimated because the number of protons crossed the crystal was not recorded in this case.

5. Calculations of PXR

The calculations of PXR characteristics from 400 GeV/c protons in the silicon crystal deflectors for the experimental conditions considered above have been performed according to the PXR kinematic theory [19]. Fig. 6 shows the angular distributions of PXR photons emitted from the QM crystal (top panel) and from the 2 mm ST crystal (bottom panel) calculated taking into account the distribution of protons across the face of the crystal as shown in Figs. 2 and 4. The PXR photons are emitted along the whole length of crystal parallel to the beam. The absorption of photons in the crystal, air and 25 μm beryllium window of the detector was considered. The angular range of the detector is shown by the square. It is seen that the main part of the PXR reflection is covered by the detector in both cases.

The calculated PXR yields for different diffraction orders as well as the ratios $I_{\gamma 1}/I_{\gamma i}$ are presented in Tables 1–3. The dependence of the detector efficiency on the photon energy was taken into account. It was calculated using the photoabsorption cross-section in silicon. The agreement of the calculated PXR yields for second and third diffraction orders with the experimental values is good for the QM crystal (Table 1). The discrepancy of about 35% for the yield of photons with E_1 is explained by their small attenuation length in silicon, which makes the calculation results very sensitive to the beam distribution across the crystal. The PXR yield discrepancy is larger for the thick ST crystal, which might be caused by a larger error in determining the number of protons that crossed

Table 2
PXR characteristics for 2 mm thick ST crystal.

Reflex	M (keV)	N_γ	I_γ (10^{-7})	$I_{\gamma 1}/I_{\gamma n}$	Theory I_γ (10^{-7})	Theory $I_{\gamma 1}/I_{\gamma n}$
1	6.46 ± 0.01	179 ± 13	3.4 ± 0.4	1	1.88	1
2	12.85 ± 0.02	101 ± 10	1.9 ± 0.3	1.8 ± 0.3	0.73	2.57

Table 3
PXR characteristics for 0.4 mm thick ST crystal.

Reflex	M (keV)	N_γ	I_γ (10^{-7})	$I_{\gamma 1}/I_{\gamma n}$	Theory I_γ (10^{-7})	Theory $I_{\gamma 1}/I_{\gamma n}$
1	6.47 ± 0.01	287 ± 17		1	5.48	1
2	12.81 ± 0.02	62 ± 8		4.6 ± 0.7	1.21	4.54

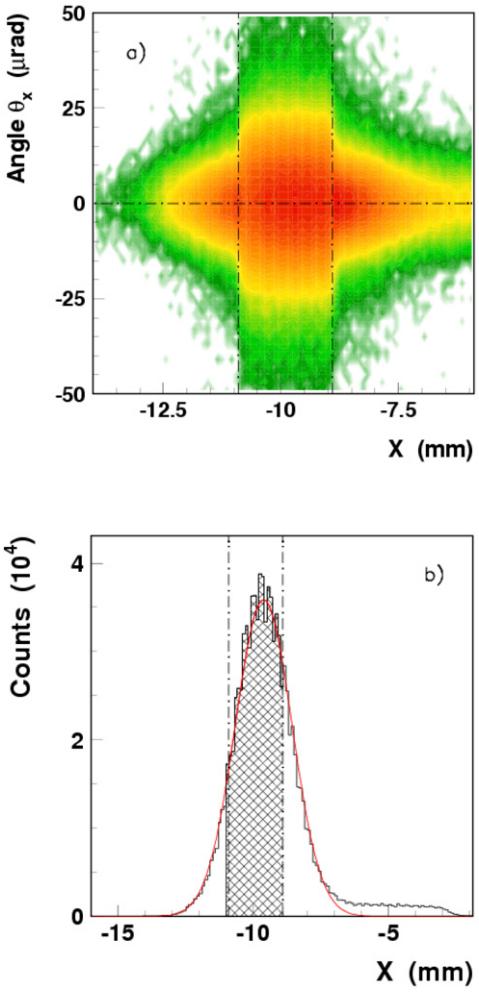

Fig. 4. (Color online.) The same as Fig. 2 for the ST crystal with 2 mm thickness. The crystal is not in a channeling orientation and deflects protons due to multiple Coulomb scattering. Both sides of the crystal are visible in (a) and indicated by dashed lines in (b).

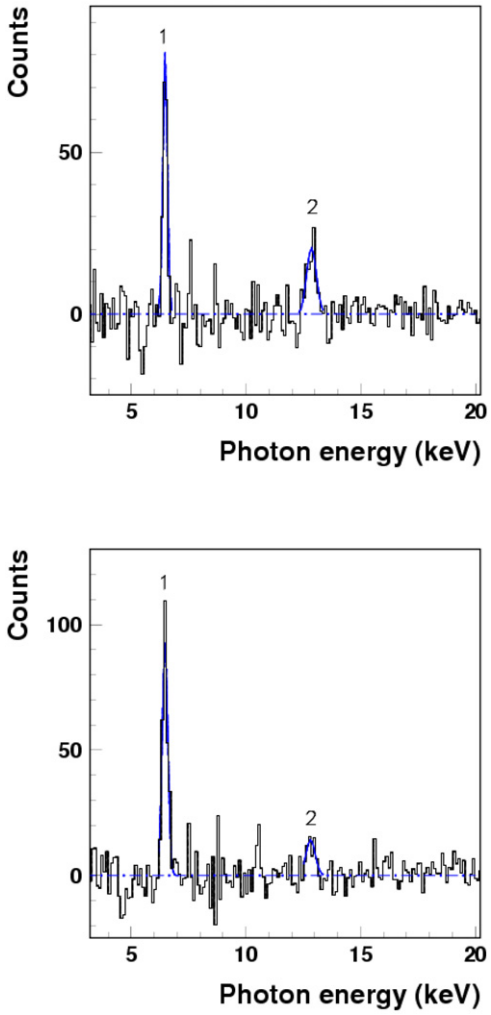

Fig. 5. (Color online.) PXR spectra produced by protons in the ST crystals with the background subtraction. Blue lines show Gaussian fits to the PXR peaks. For crystals with a thickness of 2 mm (top) and 0.4 mm (bottom).

the crystal for this measurement. The difference of the $I_{\gamma 1}/I_{\gamma 2}$ ratio is about 45% (Table 2). For the thin ST crystal there is good agreement of the $I_{\gamma 1}/I_{\gamma 2}$ ratio values (Table 3).

6. Conclusions

Our experiment allowed to observe parametric X-ray radiation from 400 GeV/c protons in bent silicon crystals aligned with the beam (in a collimation geometry). The measurement was performed for PXR photons generated by the whole incident beam. The radiation was emitted in a direction normal or close to normal to the beam. A few peaks in the X-ray spectra measured by the semiconductor silicon detector correspond well to the PXR photon energies of different diffraction orders E_n. The total yield of photons was about 10^{-6} per proton for the quasi-mosaic crystal and a little smaller for the strip crystals. It was shown that the relative yield of soft photons with the energy E_1 increases when

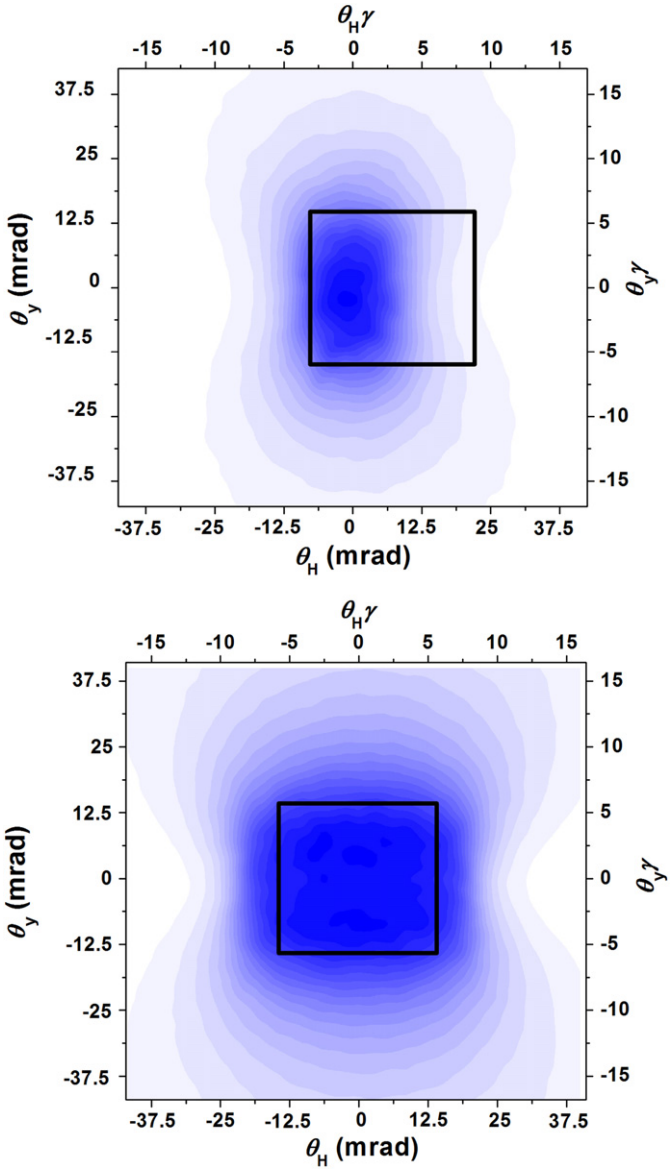

Fig. 6. (Color online.) The angular distributions of PXR photons around the reflection center calculated for the QM crystal (top) and the 2 mm ST crystal (bottom). The black square shows the angular range of the detector.

the crystal thickness intersected by the beam decreases. The good agreement of calculations with the experimental data shows that the PXR kinematic theory [1,19] is valid in bent crystals with sufficiently small curvature when the crystal bend radius R is much larger than the critical one R_c.

The intensity of PXR emitted from halo protons in a primary crystal collimator of a high-intensity circular accelerator should be sufficient to control its structure state. It should be noted that the PXR yield in the crystal inside the accelerator pipe will be larger than the values observed in our experiment due to vacuum conditions. The vacuum conditions should allow to observe also characteristic X-ray radiation of crystal atoms excited by protons. The energy of the characteristic radiation peak in silicon is 1.74 keV and its yield [10] should be comparable to the one in the PXR peaks. Furthermore, halo protons will pass through the crystal collimator very close to its surface in the case of perfect alignment. Therefore, PXR attenuation in the crystal will also be suppressed. Both these circumstances will considerably increase the yield of E_1 photons. In the case of poor crystal alignment the distribution of halo protons across the crystal collimator becomes close to uniform with a width of a few millimeters. For these orientations the relative yield of higher order photons of PXR increases. Thus, the analysis of PXR spectra recorded from halo protons crossing a primary crystal collimator gives an additional possibility to control its orientation. Other issues, such as the radiation hardness of the PXR detector are not included in our considerations.

Future experiments on PXR from high energy protons in bent crystals may be devoted to the study of the radiation yield from channeled particles and measurements of the PXR angular distribution, which is important for the above mentioned application of PXR.

Acknowledgements

We wish to acknowledge the strong support of the EN-STI group. We also acknowledge the partial support by the Russian Foundation for Basic Research Grants 05-02-17622 and 06-02-16912, the RF President Foundation Grant SS-3383.2010.2, the “LHC Program of Presidium of Russian Academy of Sciences” and the RFBR-CERN grant 08-02-91020. G. Cavoto and R. Santacesaria acknowledge the support from MIUR (grant FIRB RBFR085M0L_001/I11J10000090001 and PRIN 2008TMS4ZB). US participants supported by US DOE under the LHC Accelerator Research Program (LARP). A.S. Gogolev acknowledges the partial support through the project ADTP No. 2.1.2/13162. The Imperial College group gratefully acknowledges support from the UK Science and Technology Research Council.

References

[1] M.L. Ter-Mikaelian, High Energy Electromagnetic Processes in Condensed Media, Wiley, New York, 1972, Akad. Nauk Arm. SSR, Yerevan, 1969.
[2] G.M. Garibyan, Yan Shi, Zh. Eksp. Teor. Fiz. 61 (1971) 930, Sov. Phys. JETP 34 (1971) 1756.
[3] V.G. Baryshevsky, I.D. Feranchuk, Zh. Eksp. Teor. Fiz. 61 (1971) 947, Sov. Phys. JETP 34 (1971) 1778.
[4] A.V. Shchagin, X.K. Maruyama, in: S.M. Shafroth, J.C. Austin (Eds.), Accelerator-Based Atomic Physics: Technique and Applications, AIP Press, New York, 1997, p. 279.
[5] P. Rullhusen, X. Artru, P. Dhez, Novel Radiation Sources Using Relativistic Electrons, World Sci., Singapore, 1998.
[6] V.P. Afanasenko, V.G. Baryshevsky, R.F. Zuevsky, et al., Phys. Lett. A 170 (1992) 315.
[7] Yu.N. Adishchev, et al., JETP Lett. 81 (2005) 241.
[8] Yu.N. Adishchev, et al., Nucl. Instrum. Methods B 252 (2006) 111.
[9] A.V. Shchagin, V.I. Pristupa, N.A. Khizhnyak, Phys. Lett. A 148 (1990) 485.
[10] A.V. Shchagin, JETP Lett. 80 (2004) 469.
[11] A.V. Shchagin, J. Kharkiv Univ., Phys. Ser. “Nuclei, Particles Fields” 30 (2006) 35.
[12] A.S. Gogolev, A.P. Potylitsyn, A.M. Taratin, Yu.S. Tropin, Nucl. Instrum. Methods B 266 (2008) 3876.
[13] W. Scandale, et al., Phys. Lett. B 692 (2010) 78.
[14] Yu.M. Ivanov, A.A. Petrunin, V.V. Skorobogatov, JETP Lett. 81 (2005) 99.
[15] S. Baricordi, et al., Appl. Phys. Lett. 91 (2007) 061908.
[16] S. Baricordi, et al., J. Phys. D: Appl. Phys. 41 (2008) 245501.
[17] M. Pesaresi, W. Ferguson, J. Fulcher, G. Hall, M. Raymond, M. Ryan, O. Zorba, JINST 6 (2011) P04006, doi:10.1088/1748-0221/6/04/P04006.
[18] W. Scandale, et al., Phys. Rev. Lett. 101 (2008) 234801.
[19] H. Nitta, Phys. Rev. B 45 (1992) 7621.